Influence of Talc Genesis and Particle Surface on the Crystallization Kinetics of Polypropylene/Talc Composites

L. A. Castillo, S. E. Barbosa, N. J. Capiati

Planta Piloto de Ingeniería Química (UNS—CONICET), Bahía Blanca, Argentina

Received 29 August 2011; accepted 19 January 2012
DOI 10.1002/app.36846
Published online in Wiley Online Library (wileyonlinelibrary.com).

ABSTRACT: Talc is a laminar silicate, considered as an excellent nucleating agent for polypropylene (PP) crystallization. However, properties of PP/talc composites depend on the morphology, size, and surface of mineral particles. In this sense, talc from several ores, having different morphology, imparts specific characteristics on these materials. Also, taking into account that PP-talc adhesion is not necessarily good due to the apolar character of PP, talc surface has been modified in order to increase this parameter. In this work, the effects of talc genesis, geomorphologic aspects, and particle surface characteristics on crystallization of PP/talc composites are analyzed. Isothermal crystallization of PP/talc composites was studied by using differential scanning calorimetry, based on Avrami model. The final crystalline morphology of talc-filled PP was analyzed by means optical microscopy. The results show that the blocky talc morphology favors even more the crystallization compared to the platy one, at the same particle size. Taking into account the surface treatment studied in this work, the talc surface is made hydrophobic and the particle delamination is favored. As a consequence, so-modified talc is very effective in increasing the crystallization temperature of PP and the nuclei number that grow during the crystallization with respect to the untreated talc.
 J Appl Polym Sci 000: 000–000, 2012

Key words: composites; crystallization; kinetics; talc morphology; surface-modified talc

INTRODUCTION

The strong nucleating effect of talc on semicrystalline polymers, particularly on polypropylene (PP), has been demonstrated by different authors, increasing the industrial interest and application for this particular composite.[1–3] In talc-filled PP, the influence of these particles on PP crystallization is singular and is very different that occurs with other inorganic fillers, although having the same laminar morphology.[4–6] Studies based on X-ray diffraction confirm that talc produces a constrained crystalline structure in PP where polymer chains align regularly on the basal planes of talc particles.[7,8] Talc can initiate heterogeneous crystallization, thus changing the morphology, chain orientation, crystal type, and crystallinity degree of PP, conferring significant changes in optical, thermal, mechanical, and barrier properties of the composites.[9,10]

Usually, talc in nature is associated with different minerals, according to its genesis. Talc from several ores differs on chemical composition, type and proportion of associated minerals, and crystal morphology.[3] These aspects confer to talc specific whiteness, particle shape, oil absorption, and amphiphilic characteristics. On the other hand, they also affect thermal, mechanical, and optical properties of PP/talc composites, as they influence on PP crystallization. As a consequence, the nucleating ability of talc on PP and the crystallization behavior of composites will depend on talc geomorphologic and geochemical origin as well as the mineral processing like milling, micronization, among others.

Particularly in composite materials, proper control of the adhesion between talc and polymer matrix is important to tailor their properties. In general, stronger filler–matrix interactions result in improved ductility, strength, and surface quality.[11] As a means of controlling these interactions, minerals have been treated with appropriate surfactants.[12,13] These agents act by modifying the interfacial region between the inorganic filler and the organic polymer to provide an improved bonding between them. Also, they increase the filler dispersion in the polymeric matrix. Taking into account the high surface energy of talc particles (35–40 J/cm^2), when it is mixed with PP (surface energy = 3×10^{-6} J/cm^2), it is necessary to modify their surface to improve the interfacial adhesion. In this sense, it is desirable that the particle surface becomes more hydrophobic. Consequently, talc surface modification would lead to a change of the nucleation kinetics of PP as the filler surface interacts with the polymer during the crystallization.

Correspondence to: L. A. Castillo (lcastillo@plapiqui.edu.ar).

There are some previous studies on the crystallization behavior in PP/talc composites. They involve isothermal and non-isothermal analysis, focusing on the influence of different variables like particle concentration, surface modification, interfacial agent addition, etc. De Medeiros et al.,[14] using non-isothermal conditions in a crystallization study, concluded that the crystallinity degree and the crystallization temperature increase with the filler content and decrease at higher cooling rates. Albano et al.[15] observed that, at higher talc concentrations, a saturation phenomenon of the nucleating agent is produced during the non-isothermal crystallization of PP/talc composites. Also, they discussed that the presence of particle agglomerates would give rise to a decrease in nucleation rate. Marosi et al.[16] studied the role of a modified interfacial layer around talc particles, by elastomer addition, on crystallization behavior of PP/talc composites. They concluded that so-modified interphase reduces the nucleating ability of talc. On the other hand, Velasco et al.[8] modified talc surface with a silane treatment in order to improve the affinity between talc and PP. Their results revealed that, with a minimum amount of talc (2 wt %), an improved nucleation activity of silane-treated talc in PP is achieved.

In a previous work, acid treatments were used to improve talc purity, delamination and surface characteristics in order to be more compatible with polymers.[17] Talc of different genesis, geomorphologic characteristics, and composition were studied in order to assess and compare the effects of different acid treatments on their purification, delamination, particle size reduction, and surface modification. The main geomorphologic differences between talc samples were related with their crystalline characteristics. One of them, proceeding from Argentine, had macrocrystalline habit, with high crystallinity degree, and their particles show a typical blocky aspect.[3] The other one, from Australian ore, had platy particles with a microcrystalline morphology and low crystallinity degree. A considerable talc delamination, purification, and surface modification were achieved in both samples, but the particle size reduction was higher in platy talc. It was also demonstrated that acetate (—$OCOCH_3$) and formate (—OCOH) groups were grafted on talc surface with an appropriate organic acid treatment. Hydrochloric acid (HCl) treatment causes breakage of siloxane bonds (Si—O—Si), resulting in a particle surface with high concentration of hydroxyl groups (—OH). Talc treated with HCl behaved as neatly hydrophilic, while talc resulting from organic acid treatments was hydrophobic.

In this work, the influence of genesis, geomorphologic aspects, and surface chemistry of talc on the crystallization rate, quantity, and perfection of PP crystals in PP/talc composites is studied. Talc minerals from two different ores, having well different crystal morphologies (blocky and platy), and with and without acetic acid treatment were used. This study was performed by means of isothermal crystallization analysis and corroborated by optical observation. These analyses were done on composites with low talc concentration in order to carry out a better analysis of crystalline development, minimizing the particle interaction during crystal growing.

TABLE I
Average Particle Length (*L*) and Thickness (*e*), Determined from SEM Micrographs

Talc	*L* (μm)	*e* (μm)
A10	4.53 ± 1.65	0.139 ± 0.016
SJ10	5.85 ± 2.34	0.266 ± 0.173
A10A	2.86 ± 1.20	0.079 ± 0.156
SJ10A	4.66 ± 1.56	0.154 ± 0.223

EXPERIMENTAL

Materials and compounding

PP homopolymer Cuyolén 1102 HX (Petroquímica Cuyo, Argentine), containing a high isotacticity degree, was used as the composite matrix. Its molecular weight distribution is characterized by M_w = 303,000 g/mol, M_w/M_n = 4.45, and melt flow index = 1.8 g/mol (at 230°C).

Talc samples from two different ores of similar particle size were used: Australian talc (A10), with a purity degree of 98%, and Argentinean talc (SJ10), containing up to 16 wt % of associated minerals. Both samples were kindly supplied by Dolomita SAIC, Argentine. These minerals were surface modified with acetic acid (CH_3COOH) 99.5 % purity from Laboratorio Cicarelli (Argentine), following the method described by Castillo et al.[17] Talc name and particle size (length and thickness) are summarized in Table I.

Composites materials were prepared in a batch polymer mixer Brabender Plastograph 8356. Four different composites were prepared containing 1 wt % of each talc sample. The mixer was fed with a premixture of talc particles and PP pellets. The compounding was carried out at 185°C, under N_2 atmosphere, for 20 min at 30 rpm. Composites were named as PP'talc name'. Pure PP was processed under the same conditions in order to obtain the similar thermal history in all the samples.

Characterization

Fourier transform infrared spectroscopy (FTIR)

A Nicolet 520 Fourier transform infrared spectrometer, with a resolution of 4 cm^{-1} in transmission

mode, was used to characterize the talc samples and to follow a possible thermo-oxidative degradation evolution during composite compounding. Talc samples were diluted in potassium bromide (KBr) using two different concentrations (2 and 0.2 wt %) in order to analyze OH stretching and Si vibrations, respectively. In the case of composites, compression molded films were tested.

Scanning electron microscopy (SEM)

A JEOL JSM-35 CF scanning electron microscope, with a secondary electron detector, was used to analyze talc particle morphology. Talc dispersion and distribution in composite samples were also evaluated on cryogenically fractured surface. All samples were coated with Au in a sputter coater PELCO 91000 to make them conductive.

Optical microscopy (OM)

Crystallization process of PP/talc composites was dynamically observed in a Zeiss optical microscope under crossed polarizer. For this purpose, thin pressed composite films were melted at 200°C and then were cooled at air. Using the Leica software, photographs were acquired at different times to observe the evolution of PP crystallization.

Differential scanning calorimetry (DSC)

Isothermal crystallization experiments were carried out at different temperatures (T_c) in a Perkin Elmer Pyris 1 differential scanning calorimeter. Approximately, 8 mg of each sample were melted at 200°C and held them at this temperature for 10 min in order to erasure the thermal history. Then, the samples were cooled at T_c, using the maximum cooling rate allowed by the equipment, to reduce any non-isothermal effect which could cause errors in the thermal curves. Samples were maintained at this temperature during certain time to complete the matrix crystallization. This experimental time was determined by trial and error (30 min). Seven T_c values were chosen from the crystallization curve in non-isothermal conditions for PPA10 using a cooling rate of 10 °C/min. These values ranged between 110 and 130°C, as shown in the thermogram of Figure 1. After the isothermal crystallization, samples were heated up to 200°C to obtain the melting temperature.

RESULTS AND DISCUSSION

Talc and composites characteristics

The present study is focused to analyze different particle aspects on the nucleation and growing steps in the PP crystallization of PP/talc composites. In this way, all composites were prepared with the same talc concentration (1 wt %). Initially, results were related to filler characteristics and the particle dispersion and distribution in PP.

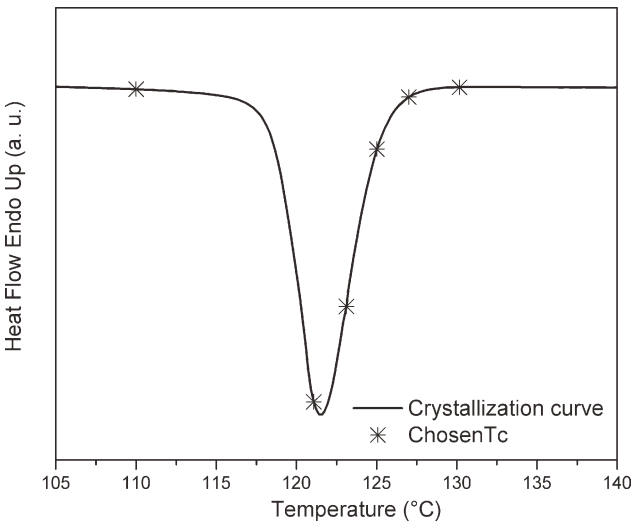

Figure 1 Non-isothermal crystallization thermogram for PP/A10 composite. Temperatures chosen for isothermal crystallization analysis are marked.

Filler aspects to be considered in the crystallization of PP/talc composites are genesis (purity and crystallinity degree), geomorphologic aspects, and surface characteristics. Initially, a brief characterization of the studied talc samples is presented. A10 and SJ10 talc proceed from two different ores; consequently they have different morphologies, as shown in Figure 2. A10 is a platy talc sample, having two types of particle which differ in size.[18] The larger ones [Fig. 2(a)] present rounded shape and they are organized in laminar concentric domains (onion-like). These particles tend to disaggregate upon milling, giving the laminar smaller ones observed in the same micrograph. On the other side, SJ10 is a blocky-type talc sample. Its particles appear as blocks, with abrupt and well defined borders [Fig. 2(b)].

The acid treatment favored the particle size reduction, delamination, and disaggregation of concentric domains [Fig. 2(c,d)]. In both talc samples, particle thickness were so reduced, but particle length was more affected in A10 (see Table I). This behavior was a result of the onion-like morphology of this talc.[17] The composition of initial and modified particle talc was studied by FTIR. The spectra of all the samples are presented in Figure 3. In A10 spectrum, only a small amount of associated minerals, as dolomite ($CaMg(CO_3)_2$) and chlorite, is present. This is expected because this talc has a high purity degree. However, SJ10 is a low-grade talc sample as it is revealed in the spectrum of Figure 3. The amount of chlorite and carbonates, like dolomite, calcite

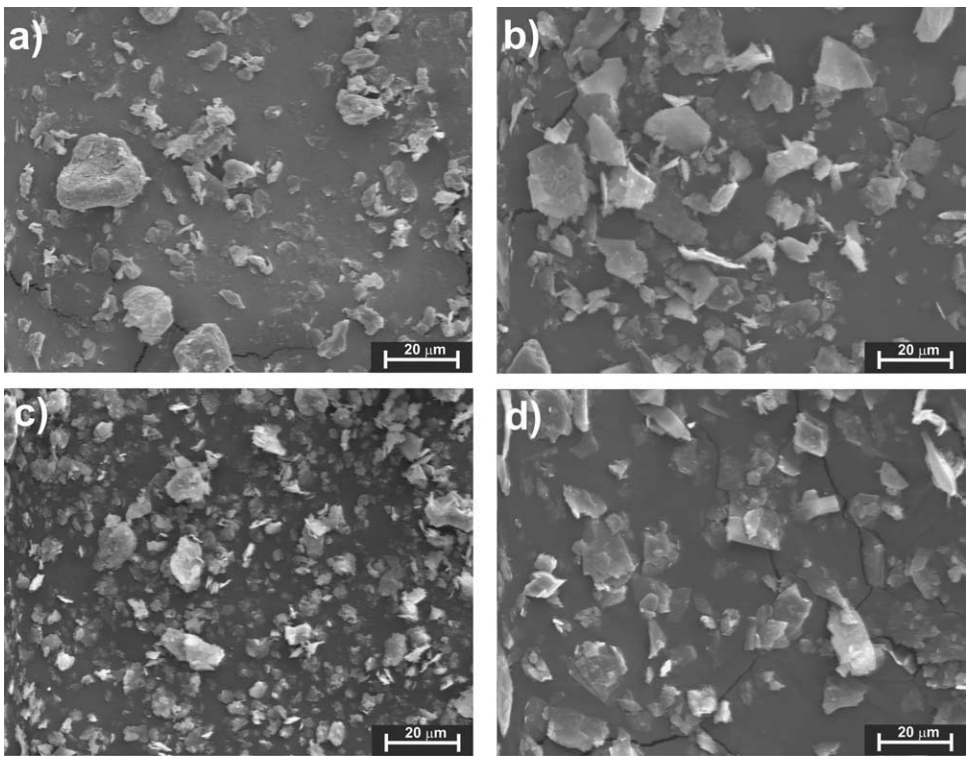

Figure 2 SEM micrographs (1000×) of talc particles: (a) A10, (b) SJ10, (c) A10A, and (d) SJ10A.

($CaCO_3$), and magnesite ($MgCO_3$), is greater than in A10, as it is shown by the relative height of the corresponding bands.[17]

Concerning to the surface modified talc, it is supposed that the organic groups from acid are bonded to the OH groups of talc. Also, the associated minerals are eliminated partially by this acid treatment. All these changes are clear by comparing FTIR spectra of modified talc to the initial one, respectively (Fig. 3). A new band in A10A and SJ10A at 2850–2950 cm^{-1}, corresponding to the organic groups grafted (—$OCOCH_3$), appears. There is a reduction in the band intensities of associated minerals (chlorite and carbonates) due to the treatment with CH_3COOH. However, none of the modified talc is free of impurities after the acid treatment.

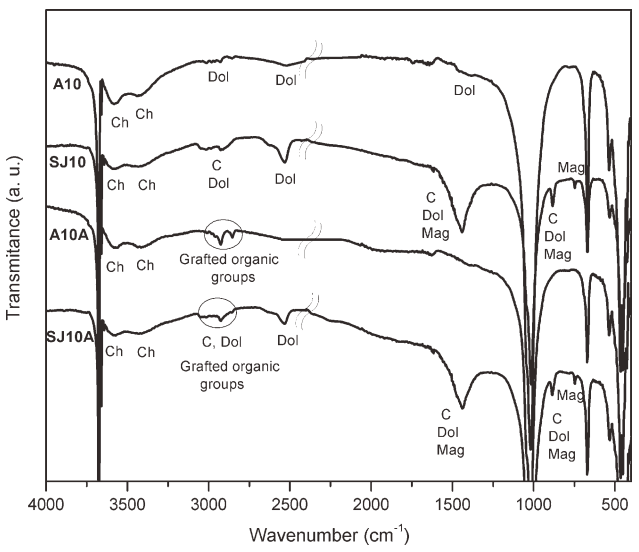

Figure 3 FTIR spectra of untreated and treated talc. Ch: chlorite, C: calcite, Dol: dolomite, Mag: magnesite.

The analysis of filler dispersion and distribution in PP matrix is a fundamental step to avoid the influence of the particle interaction or association in the crystal nucleation and growth. This control was performed by analyzing SEM micrographs of cryogenically fractured surfaces of composites. The micrographs of the samples are presented in Figure 4. Talc particle dispersion is good in all the samples, the presence of agglomerates is not observed. Also, the distribution seems to be homogeneous, as a result of exploring the entire fractured surface. The micrographs reveal a preferred orientation of talc particles, with their basal sheet planes mostly parallel to the mould surface. This characteristic organization is a consequence of the plate-like structure of talc. These results were confirmed by OM as it will be shown later.

Isothermal crystallization study

The effect of temperature on the crystallization of PP/talc composite can be observed in the isothermal curves, as it shown for PPA10 in Figure 5. With increasing the crystallization temperature, the

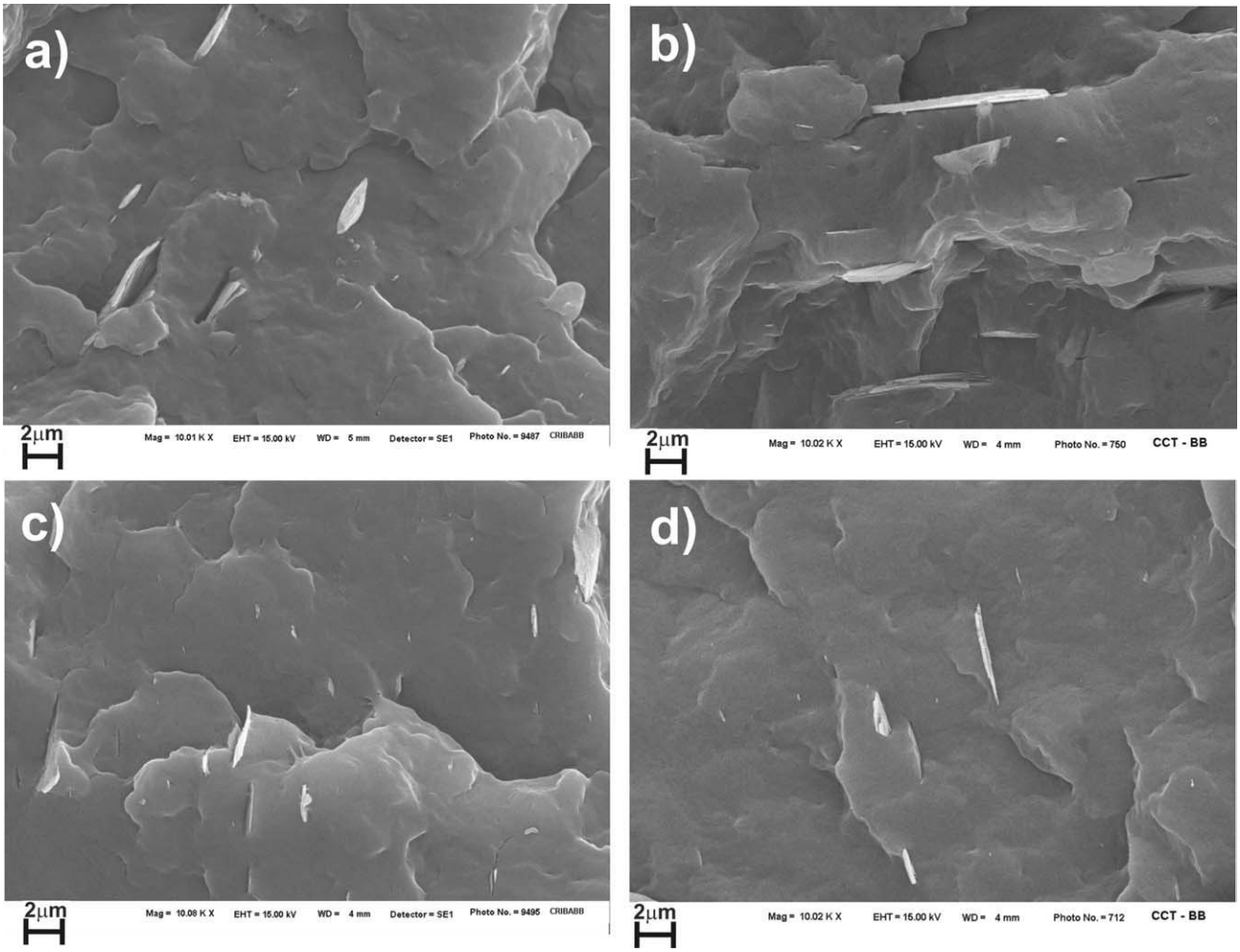

Figure 4 SEM micrographs (10,000×) of composites: (a) PPA10, (b) PPSJ10, (c) PPA10A, and (d) PPSJ10A.

exothermic peak shifts to longer times and becomes flatter. So, it means that the overall crystallization time is lengthened and the crystallization rate decreases with increasing T_c. This behavior agrees with the kinetic theory of crystallization. An increase of the crystallization temperature results in a

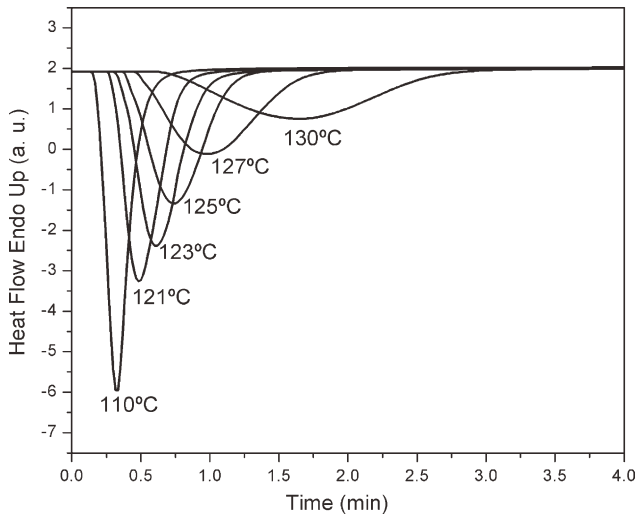

Figure 5 Isothermal crystallization curves of PPA10 composite at different crystallization temperatures.

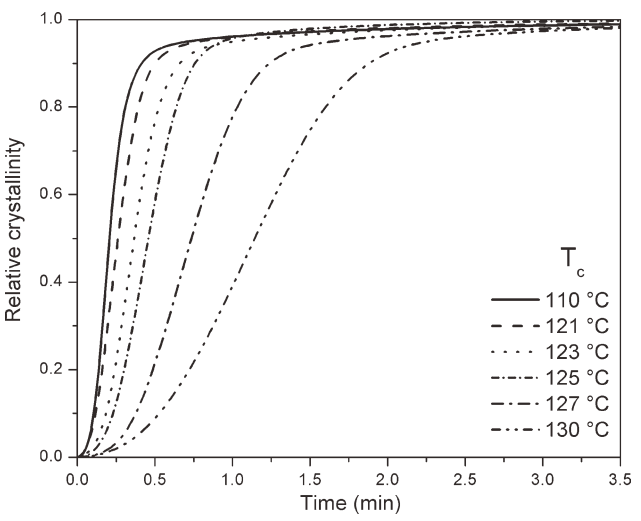

Figure 6 Relative crystallinity for PPA10 composite as a function of time, at different crystallization temperatures.

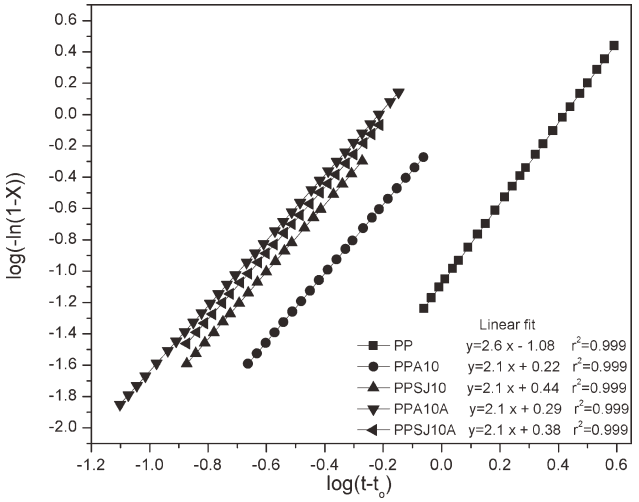

Figure 7 Linear fit of logarithmic curves of PP and PP/talc composites at 127°C.

decrease in supercooling ($\Delta T = T_m - T_c$, T_m = melting temperature) and, as a consequence, the reduction of the crystal growth rate.

The relative crystallinity as a function of time at different crystallization temperatures is shown for PPA10 in Figure 6. From these curves, it is clear that, in general, T_c influences on the crystallization kinetics of the composites. The isotherms present a sigmoid form which is characteristic of the polymer crystallization. The initial stage, corresponding to the induction time, is directly related with the impingement to the formation of stable crystalline nuclei. This induction time is reduced with high supercooling (lower crystallization temperatures), as a consequence of the diminution of critical size of the crystalline nuclei. In a second stage, a great development of crystalline mass is produced. It is important to remark that PP and the other composites presented the same behavior, but the curves are not included.

Avrami equation was used to describe the isothermal crystallization kinetics of PP and PP/talc composites using the following expression:

$$X(t) = 1 - \exp(-kt^n) \quad (1)$$

where $X(t)$ is the relative crystallinity, n the Avrami index, and k, the crystallization rate constant.[19] The plots of $\log(-\ln(1 - X(t)))$ versus $\log(t - t_o)$ for all composites at 127°C are shown in Figure 7, where t_o is the initiation time of the crystallization process. From the slope and intercept of the linear fit of these graphs, Avrami index "n" and the overall crystallization rate constant "k" are obtained, respectively. Avrami index is defined as $n = \gamma + \lambda$, where γ represents the nucleation step, which is 0 for constant nucleation (density of the nucleation site remains constant) and 1 for the sporadic nucleation. The term λ represents the growth step and it takes the value 1 for lineal development, 2 for discs, and 3 for spheres.[20]

The values of n and k for PP and composites, at different crystallization temperatures, are presented in Table II. In all the cases, the fitting was so good, having r^2 around 0.999. The values of n vary within the range of 2.5–2.9 for pure PP and 1.8–2.3 for composites, depending on the crystallization temperature and the talc type. According to previous studies, the fractional values of n can be assigned to different spatial growth of crystals, depending on their value.[21] For PP, n is equal to or greater than 2.5 indicating that the dominant crystal morphology is spherulitic, as expected. However, the values of n for composites are less than 2.3, in agreement with the idea that the main morphology is two-dimensional because talc particles nucleate PP crystallization. These results coincide with those obtained by other authors for the incorporation of clay particles in semi-crystalline polymers.[21,22] This behavior is also expected due to the laminar talc shape, from which transcrystallinity development can occur.[11]

Notable differences are observed when the rate constant of PP and PP/talc composites are considered. This kinetic parameter tends to decrease with the increase of crystallization temperature, as expected. Particularly, there is a neat increment in k values for PPA10 with respect to pure PP. In

TABLE II
Avrami Index (n) and Crystallization Rate Constant (k) of PP and PP/Talc Composites at Different Crystallization Temperatures

	PP		PPA10		PPA10A		PPSJ10		PPSJ10A	
T_c	n	k	n	k	n	k	n	k	n	k
110	2.5	28	2.3	40	2.1	48	2.2	38	2.3	47
121	2.5	2.3	2.2	13	2.2	9.0	2.3	9.2	1.8	9.8
123	2.4	0.84	2.3	11	1.9	5.2	2.2	8.4	2.5	7.0
125	2.5	0.25	2.2	4.6	1.9	4.2	2.3	4.6	2.1	3.6
127	2.6	0.083	2.1	1.7	2.1	2.8	2.1	1.9	2.1	2.4
130	2.9	0.006	2.3	0.51	2.1	0.60	2.3	0.56	2.2	0.59

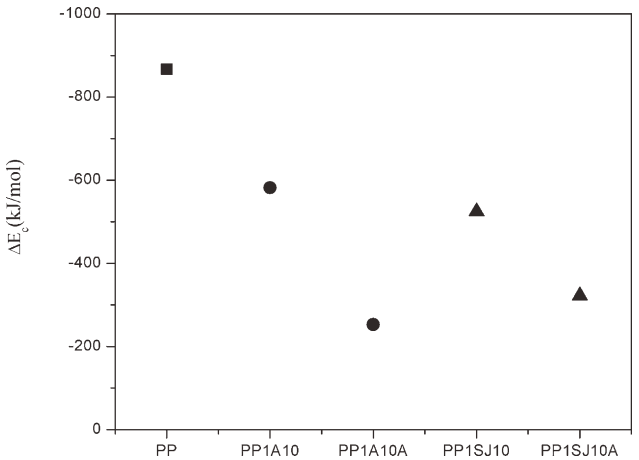

Figure 8 Activation energy for PP and PP/talc composites crystallization.

general, there is a decrease in this parameter for PPA10A when is compared to PPA10. The reason could be explained by the organic groups grafted to the treated talc surface which confine and restrict the movement of the molecule chains toward the crystal lattice. As a result, the crystal growth is stopped, and thus, the overall crystallization rate is reduced. However, there is no difference between the values of k for PPSJ10 and PPSJ10A, demonstrating that the same treatment applied on SJ10 has different effect on the crystallization behavior of the final composite.

Taking into account that the crystallization rate constant is thermally activated, the dependence of k on the temperature can be expressed as:

$$k = k_0 \exp\left(\frac{-\Delta E_c}{RT_c}\right) \tag{2}$$

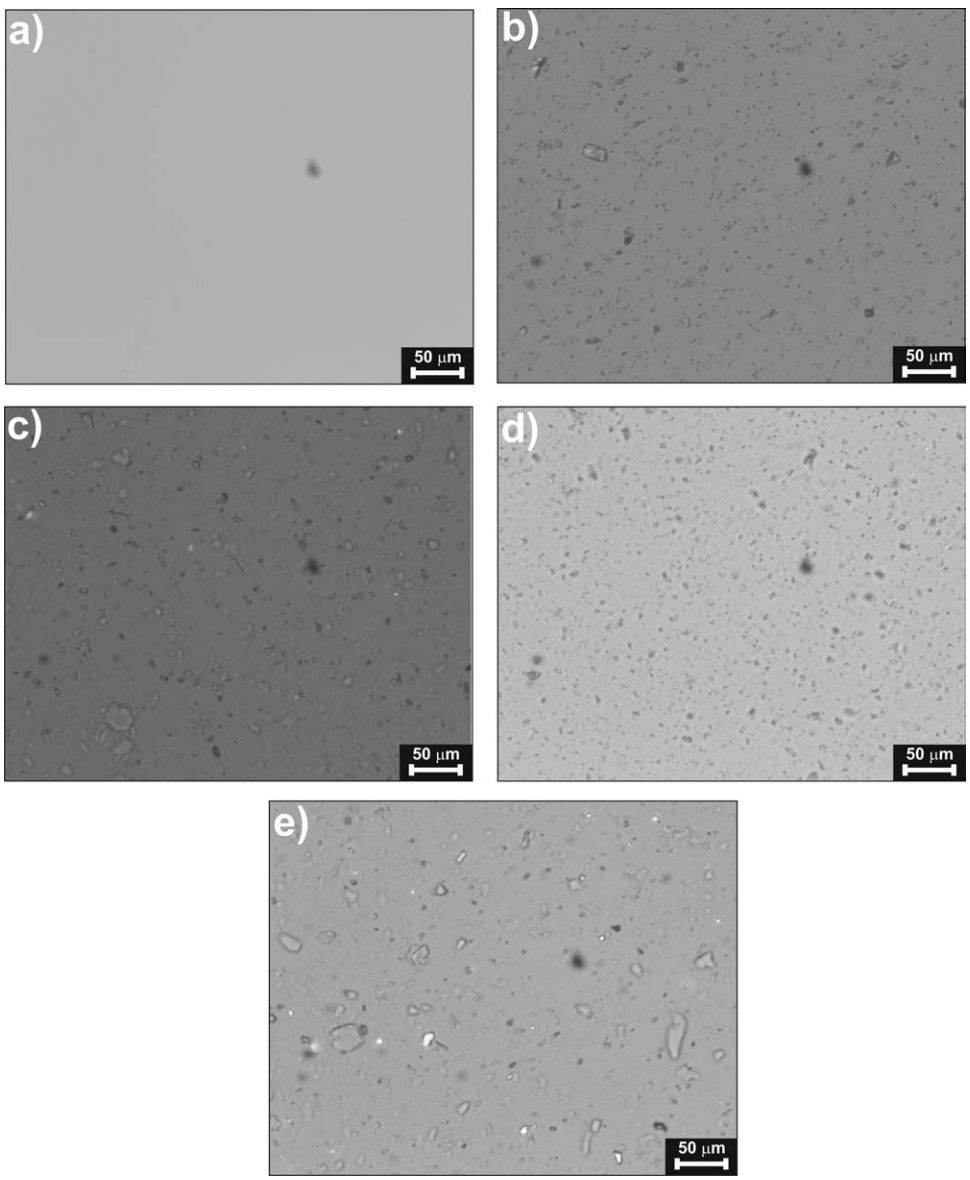

Figure 9 Optical micrographs (160×) of: (a) PP, (b) PPA10, (c) PPSJ10, (d) PPA10A, and (e) PPSJ10A in molten state.

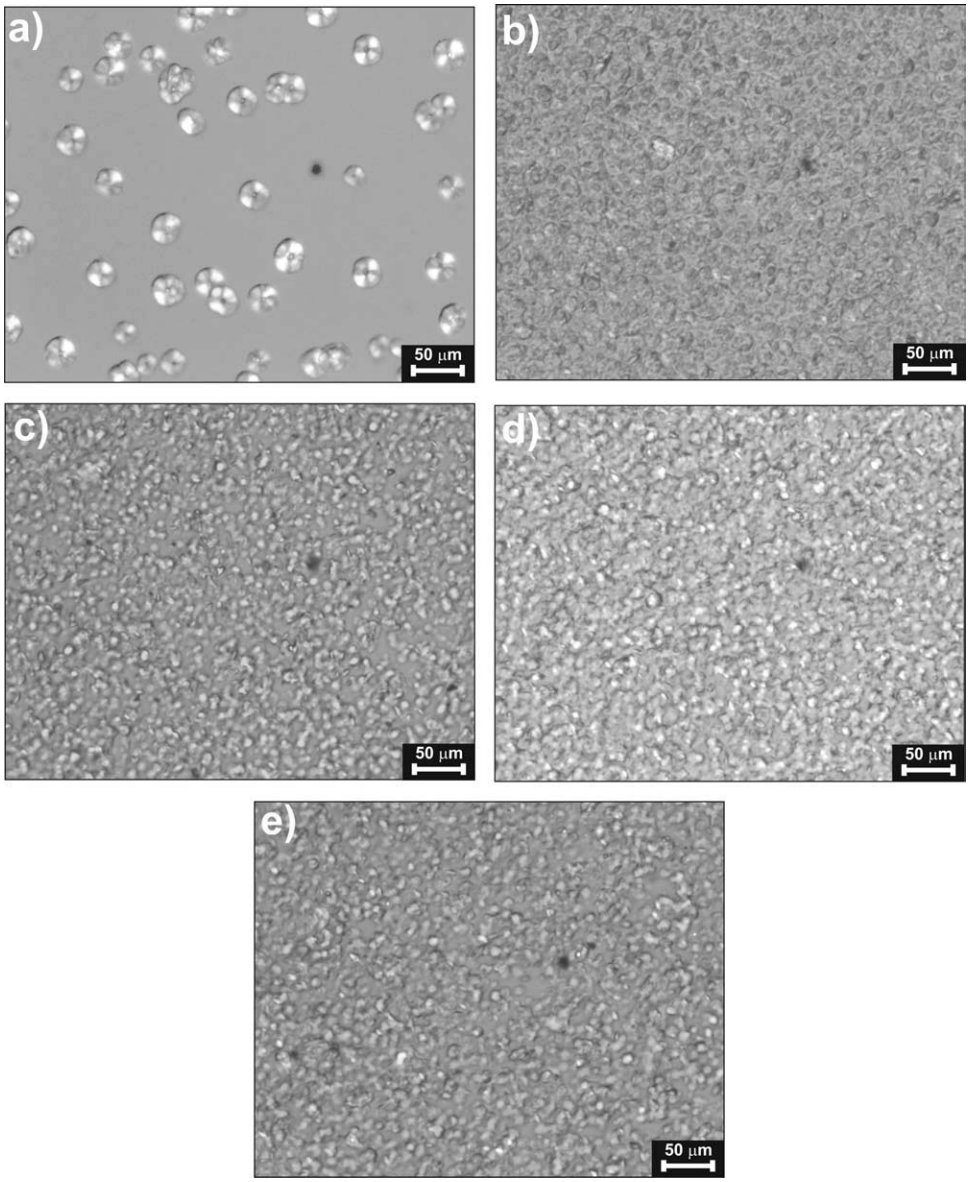

Figure 10 Optical micrographs (160×) of: (a) PP, (b) PPA10, (c) PPSJ10, (d) PPA10A, and (e) PPSJ10A after cooling for 5 min at room temperature.

where k_o is a pre-exponential constant, ΔE_c is the crystallization activation energy, R is the gas constant, and T_c is the absolute crystallization temperature.[23] From this equation, the activation energy for this process can be obtained. The values for all the specimens are plotted in Figure 8. It is important to note that this equation fit the data very well, with r^2 higher than 0.98.

Talc presence in composite implies a decrease in ΔE_c with respect to pure PP. The blocky morphology of SJ10 talc favors even more the crystallization than A10 (platy morphology), taking into account that ΔE_c was reduced 40% in the first case, against 33% for the second with respect to PP. Note that in both cases, the talc particle size is similar. However, SJ10 talc is much more crystalline than A10, which would lead to rigid particles and flat surfaces that quickly induce PP crystallization. Moreover, the activation energy decreases even more in composites containing treated talc: 71% for PPA10A and 63% in the case of PPSJ10A with respect to pure PP. Note that this decrease is greater for composites prepared with A10A than SJ10A. Taking into account that the acid treatment makes hydrophobic the particle surface and produces delamination, it is expected that the overall increase in the crystallization rate would be consequence of the increment of nuclei number. In addition, due to the platy morphology of A10, whose particles are organized in layers as "onion," it more delamination is favored during the acid treatment. This fact justifies the difference of ΔE_c values for composites with treated and untreated talc. As

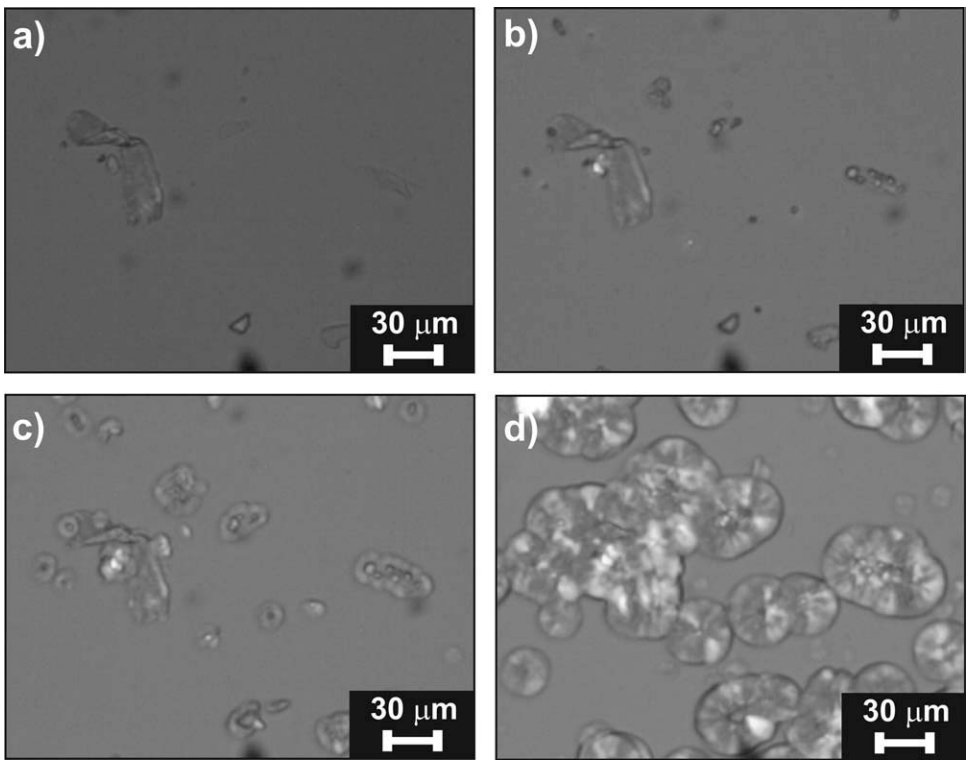

Figure 11 Optical micrographs of the PP crystal growth on the surface SJ10 talc after (a) 0, (b) 1, (c) 2, and (d) 4 min.

the crystallinity degree does not vary significantly from the untreated to treated talc composites, this difference can be also attributed to the change of particle surface energy on the type of induced crystal.[24]

Morphology and crystallization behavior relationship

Studies by OM were carried out in order to corroborate the previous results. Figures 9 and 10 show the optical micrographs of PP and PP/talc composites, including images of the molten state and after cooling for 5 min, respectively. In the case of PP, it is observed the development of typical three-dimensional spherulites, which are uniformly distributed throughout the sample.

When 1 wt % of talc is added, a larger number of spherulites were observed in comparison to PP sample. In molten composite samples, well dispersed talc particles are distinguished, confirming, at larger scale, as observed by SEM. Both samples, PPA10 and PPSJ10, are characterized by very small spherulites compared to pure PP. It is clear that talc particles can induce a large concentration of PP crystallites. As a consequence of their uniform dispersion, they produce a final material characterized by a homogeneous texture. Also, the spherulite shape seems to be changed with talc incorporation. These observations can be related to the n values obtained from the Avrami equation for PP and PP/talc composites. Values of Avrami index reported for pure PP (Table II) are equal or higher than 2.5 and, as a consequence, the main crystalline morphology is spherulitic. This result agrees with previous works.[11] However, the n values for composites are lower than PP, with an average around 2, indicating a possible two-dimensional morphology. PP mainly crystallizes following the laminar shape of talc particles.[6] Taking into account the differences between A10 and SJ10 talc morphology, it is expected a different induction in PP crystal morphology.

The induced morphology by treated talc on PP is different than the untreated one. The reason of this behavior is the greater amount of particles in PP/treated talc than to the PP/untreated ones, at the same concentration. It should be noted that the treatment favors talc delamination, increasing the number of nucleation sites.

The morphology of PP lamella growing from talc surface and the transcrystallinity were also analyzed with more details. In order to observe the location of the first crystallites, optical micrographs of PP crystallization on talc particles were taken. For this experience, a film of PP was placed onto SJ10 talc particles, being melted and after cooled (Fig. 11). Crystallization starts on talc surface much earlier than in the bulk. After 1 min, the nucleation at the

talc surface is observed as spots. Then, a relatively thick transcrystalline interfacial structure, which involves a perpendicular crystal growing from the talc surface, gradually appeared around a talc particle, until the spherulites formed through homogeneous nucleation in the bulk stop the further growth. This confirms that the presence of talc particles causes an increase of nuclei density.

CONCLUSION

From the comparative isothermal crystallization study and the optical micrograph analysis of PP and composites, prepared with treated and untreated talc of different genesis, the following conclusions can be obtained:

- PP crystallizes in a spherulitic morphology, while all the composites crystallize in bi-dimensional morphology.
- SJ10 particles induce more marked bi-dimensional morphology in PP than A10 due to the larger individual particles of the first, as a consequence of its genesis.
- Treated talc induces more bi-dimensional crystal morphology than the untreated one because the talc treatment favors the particle delamination.
- In all cases, composites crystallize with higher rate than PP because talc acts as heterogeneous agent nucleating.
- The blocky morphology of SJ10 talc favors even more the crystallization than A10 (platy morphology), taking into account that ΔE_c was reduced 40% in the first case, against 33% for the second with respect of PP.
- The activation energy decreases even more in composites containing treated talc: 71% for PPA10A and 63% in the case of PPSJ10A with respect to PP. The acid treatment makes hydrophobic the particle surface and produces delamination. In this sense, it is expected that the overall increase in the crystallization rate would be due to the increase in the nuclei number.
- These conclusions were confirmed with visual evidence given by OM.

References

1. Menczel, J.; Varga, J.J Therm Anal 1983, 28, 161.
2. Fujiyama, M.; Wakino, T.J Appl Polym Sci 1991, 42, 2739.
3. Xhantos, M. Functional Fillers for Plastics; Wiley-VCH Verlag GmbH & Co. KGaA: Weinheim, 2005.
4. Chen, Z.; Finet, M. C.; Liddell, K.; Thompson, D. P.; White, J. R.J Appl Sci 1992, 46, 1429.
5. Morales, E.; White, J. R.J Mater Sci 1988, 23, 3612.
6. Ferrage, E.; Martin, F.; Boudet, A.; Petit, S.; Fourty, G.; Joufret, F.; Micoud, P.; de Parseval, P.; Salvi, S.; Bourgerette, C.; Ferret, J.; Saint-Gerard, Y.; Buratto, S.; Fortune, J. P.J Mater Sci 2002, 37, 1561.
7. Chatterjee, A. M.; Price, F. P.J Polym Sci Polym Phys Ed 1975, 13, 2385.
8. Velasco, J. I.; De Saja, J. A.; Martínez, A. B.Revista de Plásticos Modernos 1996, 477, 271.
9. Tiganis, B. E.; Shanks, R. A.; Long Y.ANTEC '96 1996, 2, 1744.
10. Alonso, M.; Gonzalez, A.; De Saja, J. A.Plast Rubber Comp Proc Appl 1995, 24, 131.
11. Pukánsky, B. In Polypropylene: Structure, Blends and Composites; Karger-Kocsis, J., Ed.; Chapman &. HaH: London, 1995; Vol. 3, Chapter 1.
12. Schlumpf, H. P.Synthesis 1981, 12, 31.
13. Nakatsuka, T.Polym Sci Technol 1985, 27, 51.
14. de Medeiros, E. S.; Tocchetto, R. S.; de Carvalho, L. H.; Santos, I. M. G.; Souza, A. G.J Therm Anal Calorim 2001, 66, 523.
15. Albano, C.; Papa, J.; Ichazo, M.; González, J.; Ustariz, C.Compos Struct 2003, 62, 291.
16. Marosi, Gy.; Lágner, R.; Bertalan, Gy.; Anna, P.; Tohl, A.J Therm Anal 1996, 47, 1163.
17. Castillo, L. A.; Barbosa, S. E.; Maiza, J.; Capiati, N.J Mater Sci 2011, 46, 2578.
18. Holland, H. J.; Murtagh, M. J.Adv X-Ray Anal 2000, 42, 421.
19. Avrami, M.J Chem Phys 1939, 7, 1103.
20. Gnanou, Y.; Fonatnille, M. Organic and Physical Chemistry of Polymers; Wiley: New Jersey, 2008.
21. Khunova, V.; Smatko, V.; Hudec, I.; Beniska, J.Prog Colloid Polym Sci 1988, 78, 188.
22. Kerch, G. M.; Irgen, L. A.J Therm Anal 1990, 36, 129.
23. Cebe, P.; Hong, G.Polymer 1986, 27, 1183.
24. Castillo, L. A.Tesis Doctoral, Universidad Nacional del Sur, 2010.